A Preliminary Design Framework for Performance and Noise Assessment of Urban Air Mobility Vehicles

Lima Pereira, L.T.; Wang, S.; Ragni, D.

DOI
10.2514/6.2024-3334

Publication date
2024

Document Version
Final published version

Published in
30th AIAA/CEAS Aeroacoustics Conference (2024)

Aeroacoustics Conferences
June 4-7, 2024, Rome, Italy
30th AIAA/CEAS Aeroacoustics Conference (2024)

10.2514/6.2024-3334

A preliminary design framework for performance and noise assessment of urban air mobility vehicles

Lourenço T. Lima Pereira*, Sen Wang†, and Daniele Ragni‡
Delft University of Technology, Delft, The Netherlands, 2628 CD

This work describes a multidisciplinary framework proposed for the preliminary design assessment of urban air mobility (UAM) vehicles, which includes estimations of vehicle performance and acoustic emissions. Established analytical and semi-empirical methods for aircraft design and performance are combined with estimations of tonal and broadband noise components from the multi-propeller system. The estimation of the tonal components is based on steady blade loading and thickness noise, while the estimation of the broadband component considers trailing-edge scattering of each isolated propeller. Two design architectures, specifically multicopters and tilted open rotors, are assessed in this investigation. The estimated performance and noise emissions are demonstrated and compared against the available data of existing vehicles. Subsequently, a design exploration is conducted, where key performance parameters are varied and their impact on the vehicle performance, estimated cost, power consumption, and noise emissions are evaluated. The results stress the suitability of each configuration for urban air mobility, along with the operating conditions under which each architecture performs optimally. Multicopter vehicles are lighter for small ranges and speeds and, therefore, are the optimal choice for short distances. The lower MTOM also yields lower noise emissions in takeoff and landing, facilitating integration in populated urban environments. Tiltrotors have greater efficiency at high cruise speeds and, at larger ranges, demonstrate more efficient operations and, consequently, lower noise emissions, more suitable for inter-city and large commuting distances.

I. Nomenclature

X, Y, Z	=	Aircraft coordinate system based on the wing mean aerodynamic chord
R	=	Aircraft range [km]
C_L	=	Aircraft lift coefficient
C_D	=	Aircraft drag coefficient
C_M	=	Aircraft pitch moment coefficient with respect to quarter chord of the wing
S_w	=	Aircraft wing area
N_{prop}	=	Aircraft number of propellers
V_{cruise}	=	Aircraft operation cruise speed [km/h]
SPL	=	Sound Pressure Level [dB]
PWL	=	Sound Power Level [dB]

II. Introduction

Advancements in battery and electrical propulsion technology enable new possibilities for aerial transportation. The lightweight and easy operation of electric motors allows for higher flexibility of designs, easier implementation of autonomous controls, and distribution of the sources of propulsion along the vehicle. This, combined with the improving energy density of batteries has motivated the development of small aerial-electrical vehicles that can be used to optimize urban transportation needs [1]. Example applications are delivery drones and urban air mobility vehicles (UAM) [2]. The latter has gained special attention with a growing market and a number of designs. By proposing a

*Assistant Professor, Delft University of Technology, L.T.LimaPereira@tudelft.nl, and AIAA Member.
†Postdoctoral Researcher, Delft University of Technology, and AIAA Member.
‡Associate professor, Delft University of Technology, and AIAA Member.

novel means of transportation for people within large cities, the promise of UAM lies in the possibility of large-scale operations in urban areas. These operations, however, create impacts on the environment and the communities living on the routes of these vehicles. In particular, the noise emissions from the operations are a key factor for public acceptance [3]. According to EASA [4], noise is listed as one of the main concerns of European citizens with regard to urban operations of drones and UAM vehicles.

The scenario implies that, for UAM operations to be accepted, it is crucial to keep noise emissions to a minimal level. In the aviation sector, noise emissions have always been tackled at advanced steps of the vehicle design, when detailed information about the vehicle and, especially, the propulsion system, is available. However, it is important to understand that vehicle noise emissions are largely affected by design parameters that are frozen at preliminary design stages. For example the choice of vehicle architecture, number of propellers, diameter, and RPM, can influence the resulting noise emissions significantly more than a detailed propeller shape optimization [5]. As such, considering the make-it or brake-it impact of the noise emissions on the success of UAM designs, being able to assess the acoustic emissions at a preliminary stage of the design process is crucial to facilitate vehicle integration in an urban environment.

This work explores the development of a preliminary UAM design framework with the ability to accurately assess the performance and noise emissions of a proposed design. The framework is based on a vectored thrust (tiltrotor) and multicopter architecture, and is capable of quickly assessing how variations in mission profiles, performance requirements, and architectural choices influence the performance and noise emissions of the vehicle. The results focus on the design exploration of multiple variations of both architectures, culminating in a detailed discussion of their advantages and drawbacks. A summary of the design flow, underlying theories, and main assumptions used in the design framework are provided in section III. The results of this investigation are organized into two parts: the first part is dedicated to comparing the results of this work with performance data obtained from existing vehicle designs, as detailed in section IV.A. The second part focuses on exploring the design space for both multicopters and tiltrotors (section IV.B). The exploration provides a detailed description of the characteristics of both architectures, along with a comprehensive comparison of the effect of each design choice on the operational costs, energy consumption, and subsequent noise emissions.

III. Methodology

A. Tool description

The tool developed in this work is intended to produce a feasible design of a UAM vehicle based on minimum Top-Level Aircraft Requirements (TLARs). The design tool commences with a series of input definitions from the user. The main TLARs explored in this work are aircraft range, cruise speed, number of propellers, and wing area. From the inputs, the aircraft installed power, propeller disk area, and weight are iterated using a first-order mass estimation coupled with actuator disk theory, relating empty mass (EM), propulsive efficiency, and maximum takeoff mass (MTOM). The power required from the motors for taking off and landing are varied together with the estimated vehicle MTOM following a target power-to-weight ratio, the battery capacity, and the desired range and speed. From the first estimation of aircraft mass and power, the aerodynamic performance is assessed using nonlinear lifting line theory [6] and X-Foil [7] for assessing the aerodynamic coefficients of the wing and tail. The drag from the non-lift components, e.g. fuselage, landing gear, and pylons, are estimated using semi-empirical methods, following [8].

From the estimated aerodynamic performance, a more detailed breakdown of the aircraft performance follows, in which subsystem masses are obtained following a second-order mass estimation procedure. This mass breakdown utilizes an iterative process in which the battery mass and required power are varied in order to match the desired range and cruise speed. For the required power, a combination of fixed-wing and propulsive lift is allowed, such as to create multicopter and fixed-wing-based cruise operations. The converged vehicle data is used to estimate the aircraft architecture, operation parameters, performance, and noise signature. The noise estimation encompasses both analytical and semi-empirical methodologies for assessing tonal and broadband noise emissions. In greater detail, tonal noise is assessed using Hanson's method [9] over blades that are considered lumped elements rotating at 70% of the propeller radius. Thickness, lift, and drag components are evaluated following a parabolic thickness and uniform lift and drag distribution [5]. Broadband noise estimations follow Schlinker and Amiet's method [10] and are based on trailing-edge noise emissions from the propeller blades. Required wall-pressure wavenumber-frequency spectra follow the work of Corcos [11] and are estimated using the semi-empirical models of Kamruzzaman [12] for the wall-pressure spectrum and Hu [13] for the correlation length. Accordingly, predictions are carried out considering a lumped element at 70% of the propeller radius. It is important to highlight that only the noise from the isolated propellers is assessed. Several

works [5, 14] have demonstrated the importance of propeller integration in noise signature, and further work is still required to assess the validity of the assumption. The noise emissions are evaluated over a sphere around the vehicle, which is later used for computations of sound power and propagation of the emissions to the ground.

The operating expenses (OE) are also used to discuss the market viability for each of the designs. The OE is computed following Brown and Harris[15] where direct operating costs (DOC) and indirect operating costs (IOC) are considered. Here, DOC consists of pilot cost, maintenance cost, and energy cost, where pilot cost is assumed to have an average wrap rate of around €100/h and maintenance cost is evaluated using an approximate average rate of €60/h. In addition, the maintenance time is considered for 62.5% of the flight hours [15]. The energy cost is estimated based on the average non-household electricity price in Europe, which is €0.1833/kWh as of 2023. The estimation of IOC is approximated as 40% of DOC [15].

Figure 1 illustrates the tool flowchart. The preliminary sizing tool facilitates the design process by requiring minimal input information, such as the operating range, speed, flight altitude, and number of passengers. Output data includes an automatically generated aircraft geometry that can be used to guide vehicle feasibility and provide geometric details.

Two slightly different branches of the software are used to estimate the performance of the multirotor and the tiltrotor vehicle. For the multirotor, no lifting elements are considered and the propellers are distributed equidistant from each other along two radii, following the design of the Volocopter VoloCity vehicle. The tiltrotor architecture follows the design of the Joby S4 architecture, with a V-Tail, two rotors mounted at the tip of the tails, and the remaining ones evenly mounted over the wings. The rotors are used for lift generation during takeoff and landing and for forward flight during cruise. Figure 2 shows examples of the generated vehicle architecture of both vehicles.

The vehicle mission is defined equal to both vehicle architectures. This choice enables a direct comparison between the results obtained from multicopters and tiltrotors. The mission is segmented into 6 stages including, takeoff, climb, cruise, loiter, descent, and landing. During the exploration of the design, only the cruise range (R) and speed (V_{cruise}) are varied. Cruise height is kept at 300 m (1,000 ft). Takeoff, climb, descent, and landing times and speeds are based on the works of [16, 17]. It is worth mentioning that the latter has potentially a direct relation with emitted noise in cruise, consequently influencing the aircraft performance, mission time, and energy consumption. This latter influence is to be considered in future studies. Table 1 illustrates the mission definitions and main criteria for performance assessment.

Mission stage	Duration [s]	Speed [km/h]	Distance [km]	Load factor [-]
Takeoff	45	0	-	1.0
Climb	-	2	0.3	1.1
Cruise	45	V_{cruise}	R	1.0
Loiter	120	V_{cruise}	-	1.0
Descent	-	-	0.3	1.0
Landing	45	0	-	1.0

Table 1 Breakdown of the mission stages and considerations for performance assessment.

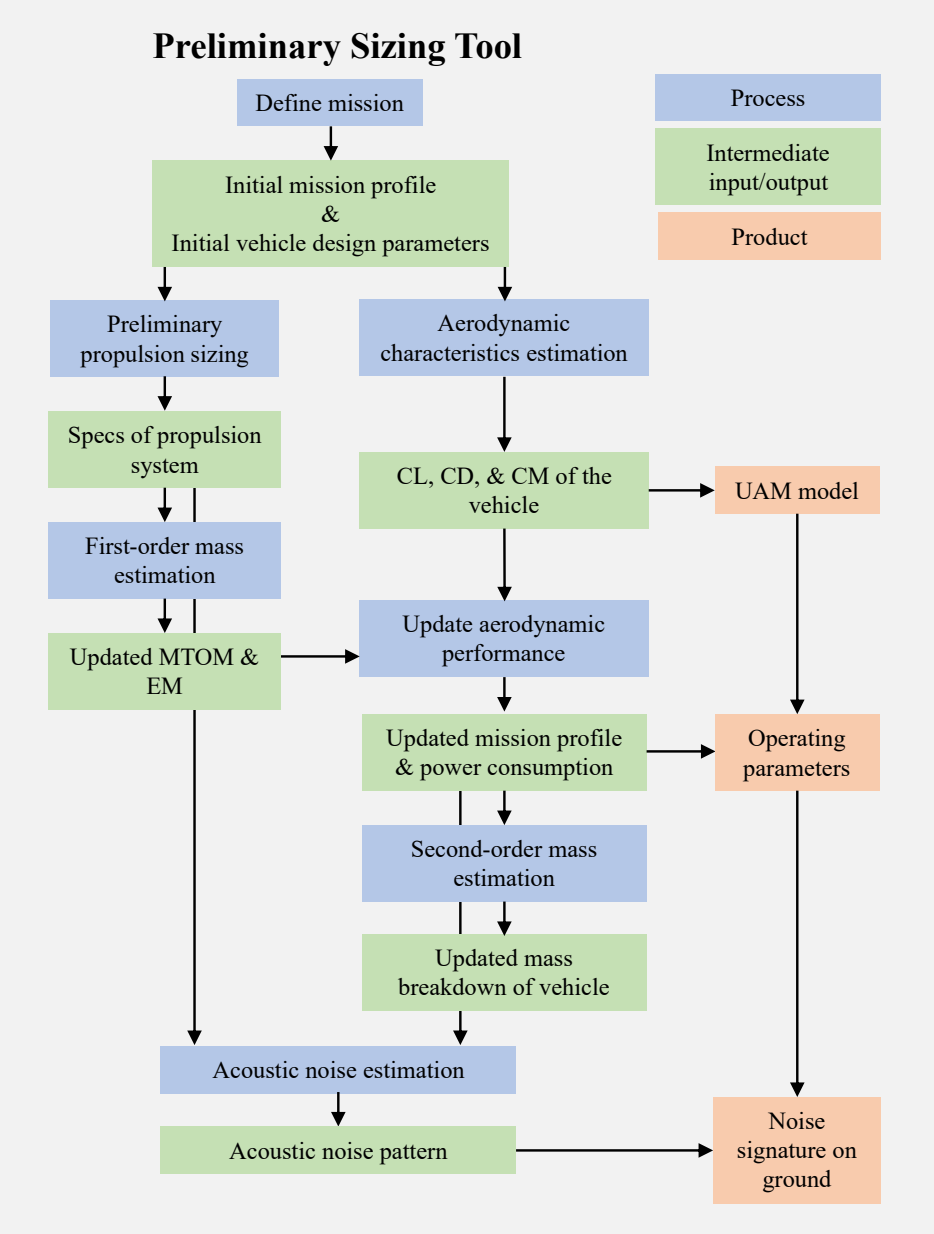

Fig. 1 Flowchart of the preliminary design tool proposed.

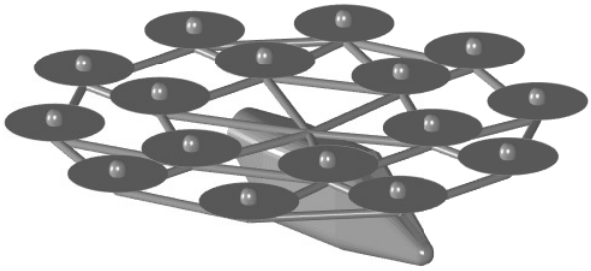

(a) Multicopter

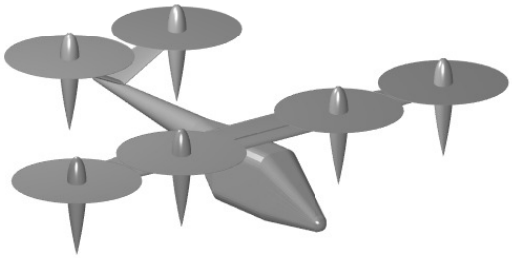

(b) Tiltrotor - takeoff and landing configuration

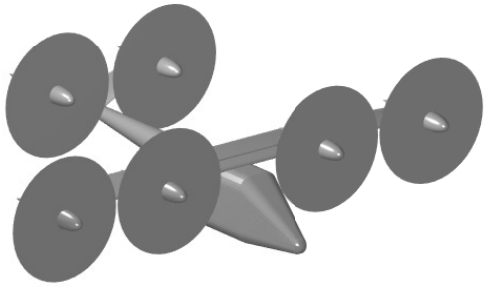

(c) Tiltirotor - cruise configuration

Fig. 2 A demonstration of vehicle architectures of (a) the multicopter, and the tiltrotor in (b) takeoff and (c) cruise configurations.

IV. Results and discussions

A. Exploration of existing vehicles platforms

This study starts with a first assessment of the reliability of the tool based on data from existing vehicle prototypes. Two vehicle designs are assessed in this section, one following the design of the Volocopter X2 vehicle, representative of a multicopter vehicle. The other one is modeled after the design of the Joby S4, which has a tiltrotor architecture. The main objective of this initial exploration is to verify that the tool can produce performance characteristics that align reasonably well with existing data for vehicles with a similar mission profile. Note that the two vehicles are designed for different missions, with the multicopter vehicle aimed for short range and small number of passengers (1 passenger), and the tiltrotor design intended for long range and higher number of passengers (4 plus a pilot).

Available information is taken from the Vertical Flight Society database on electric vertical takeOff and landing (eVTOL) vehicles [1]. It is necessary to mention that the sources and reliability of this information are not available and a discussion on the agreements and disagreements must be carried out carefully. A driving parameter to the design of eVTOL is the battery energy density. Information on the S4 model describes a pack-level density of 235 Wh/kg. In the lack of the same information for the multicopter design, the same value is used for carrying out both designs, assuming this is a reasonable energy density for a vehicle being designed currently.

At first, a comparison of the performance parameters obtained by the tool with available information on the aircraft's performance is drawn. Tables 2 and 3 show the main performance parameters used as input and received as output from the tool along with existing information on the two reference vehicles selected. Table 2 highlights the comparisons of the multicopter architecture and Table 3 of the tiltrotor one. The first 5 parameters correspond to the required inputs from the design tool, while the remainder are the main output performance parameters of the tool. The comparisons indicate the tool-output results have reasonable alignment with the data available from the reference vehicles. Trends for power, wing, and disk loading are also in agreement with the historical ones mentioned in [18], pointing to a valid comparison between multicopter and tiltrotor performances.

	Units	Predicted	Volocopter 2X reference
Number of PAX + Pilot	-	1	1
Pack-level specific energy	Wh/kg	235	-
Number of propellers	-	18	18
Range	km	27	27
V_{cruise}	km/h	90	102
Empty Mass (EM)	kg	420	290
Maximum Takeoff Mass (MTOM)	kg	540	450
Installed power per prop	kW	35	45
Propeller rotational speed in cruise	RPM	705	-
Propeller rotational speed in takeoff	RPM	701	-
Disk loading	kg/m^2	14	10
Power loading	kg/kW	15	10

Table 2 Comparison between predicted performance parameters of a multicopter vehicle from the tool and reference data from Ref. [19].

Figure 3 shows a comparative weight breakdown of total (MTOM) and empty masses (EM). As observed for both vehicles, battery weight makes up a significant percentage of the aircraft weight. Interestingly, this percentage is much higher for the multicopter vehicle, despite its range and cruise speed being significantly lower than that of the tiltrotor vehicle. Figure 4 gives more insights into this phenomenon by demonstrating the required battery energy, and consequently mass, for each mission stage. The tiltrotor vehicle, due to its efficient design for cruise, yields higher energy requirements in other stages of the mission, with a total 37% of the battery weight used for takeoff, climb, descent, and landing. The remainder 63% (reserve not included) is required for cruising over 160 km. The multicopter vehicle, however, shows low energy use during takeoff, climb, descent, and landing (lower power loading), in retrospect of an energy-demanding cruise condition (propellers required for lift and forward move). As a result, around 92% of the

	Units	Predicted	Joby S4 reference
Number of PAX + Pilot	-	4+1	4+1
Pack-level specific energy	Wh/kg	235	235
Wing span	m	10.7	10.7
Range	km	160	160
V_{cruise}	km/h	250	300
Empty Mass (EM)	kg	1,850	1,950
Maximum Takeoff Mass (MTOM)	kg	2420	2450
Installed power per prop	kW	172	236
Propeller rotational speed in cruise	RPM	244	-
Propeller rotational speed in takeoff	RPM	830	-
Wing loading	kg/m^2	169	171
Power loading	kg/kW	2.3	1.7

Table 3 Comparison between predicted performance parameters of a tiltrotor vehicle from the tool and reference data from Ref. [20].

vehicle battery, ($\approx 65\%$) of its empty mass is dedicated to batteries required for cruising 27 km.

The resulting noise emissions are shown in Figure 5, which depicts the overall emission spectrum for each of the vehicles during takeoff and cruise. The corresponding sound power levels are summarized in Table 4, with and without human perception (A-weighting based) applied. Figure 5 shows the estimated tonal and broadband spectra of both aircraft. The figures highlight some of the distinctive features of UAM eVTOL designs with respect to conventional single or twin-engine propeller-driven vehicles, i.e., the dominance of the high blade passing frequency (BPF) harmonics and broadband on the A-weighted noise level. The large rotors and, consequently, low RPMs required for takeoff and landing combined with large solidity and number of blades for some designs, yield very low frequencies and levels on the first BPFs (lower than 100 Hz), which are usually neglected when humans perception is taken into account. This points to a fundamental role of broadband and high-BPF components in the total noise emissions. The latter two are more challenging to address at preliminary design stages as they require particularly detailed information on the blade loading distribution, turbulence intensity, and boundary-layer characteristics at the trailing edge of the blades. For example, the current design framework considers lumped force and scattering noise from the propellers and neglects the contribution of incoming turbulence on the noise emissions. Thus, predictions on noise should always be interpreted on a global scale and, most likely, improvements are required when detailed noise emissions are sought.

Table 4 summarizes the sound power emissions estimated for each vehicle. The table reveals that the vehicle architecture choice has an important influence on the noise emissions at different mission stages. Multicopter vehicles use the propellers for lift generation during both takeoff and cruise. The required power and rotational speed of the propellers are higher during cruise than during takeoff. As a consequence, noise emissions will be higher during the cruise than during takeoff and landing. Conversely, tiltrotor vehicles utilize wing-based lift during cruise, which yields a much lower power and rotational speed during cruise. The noise emissions at cruise stage are therefore notably lower. The overall sound power emissions (in dB(A)) point to a similar level of emissions for the two vehicles, where the tiltrotor vehicle is able to carry 4 passengers against 1 of the multicopter. In addition, the table suggests that the dominant components in noise emissions of the tiltrotor and multicopter architectures are broadband and tonal, respectively.

The directivity of the emitted noise is shown in Figure 6, which displays the sound pressure level over a 10-meter-radius sphere surrounding the vehicle. As shown in Figure 6 (a), the emitted sound from the multicopter architecture is maximum towards the upstream and downstream directions (along the Z-plane) and minimum towards the ground. This is due to the rotor disks mainly normal to the gravity direction. The work of Monteiro et al. [14] has demonstrated how unsteady loading can affect this directivity patterns, leading to higher noise emitted towards the ground, which contradicts the result of Figure 6 (a). On the other hand, cruise configurations of the tiltrotor architecture are dominated by broadband noise, which has a less polarized directivity pattern than tonal noise. The impact of unsteady loading on the directivity pattern is therefore not as obvious as observed in Figure 6 (b). In the selected range of SPL shown in Figure 6 (c), the directivity pattern is seen as almost omnidirectional.

The results from this section show that the design tool can coherently assess the performance of the two design

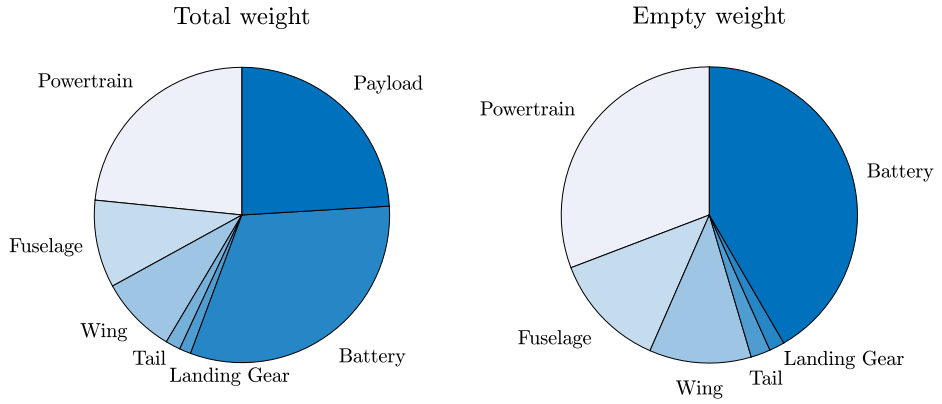

(a) Multicopter

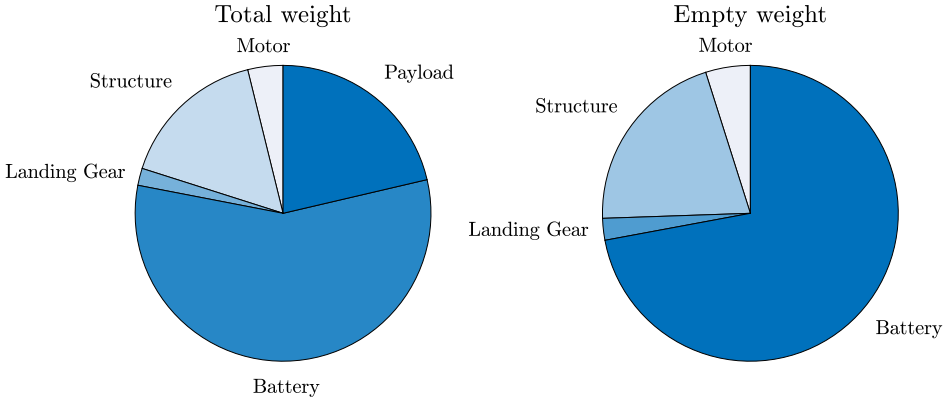

(b) Tiltrotor

Fig. 3 Breakdown of estimated component masses for the (a) multicopter, and (b) tiltrotor architectures.

	Units	Multicopter		Tiltrotor	
		Takeoff	Cruise	Takeoff	Cruise
Overall Sound Power Level	dB	124	125	134	86
	dB(A)	82	82	112	85
Overall Tonal Sound Power Level	dB	124	124	134	54
	dB(A)	81	81	112	4
Overall Broadband Sound Power Level	dB	74	76	89	86
	dB(A)	74	76	89	85

Table 4 Summary of noise emissions estimated for both multicopter and tiltrotor reference vehicles.

architectures as intended. Discrepancies with reference vehicles/theories and concerns from oversimplifications are noticed. However, the issues are mostly seen to affect the noise directivity and are highly sensitive to the detailed design of the propulsive systems and battery energy density. The following section is dedicated to exploring the use of the framework to study the influence of a series of design choices on the performance and noise emissions of the vehicle.

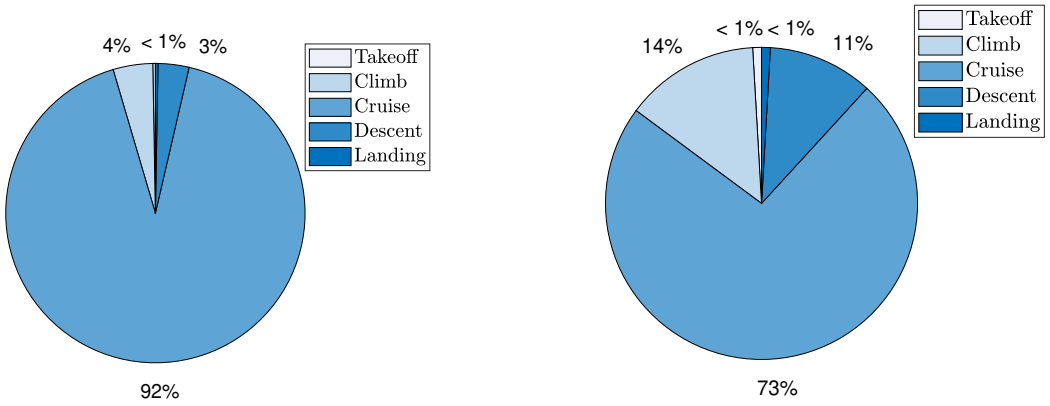

(a) Multicopter

(b) Tiltrotor

Fig. 4 Breakdown of battery requirements for different stages of the aircraft mission. (a) multicopter and (b) tiltrotor architectures.

B. Design exploration for multicopter and tiltrotor vehicles

An extended assessment of the design tool is carried out by conducting a design exploration considering both architectures. For the assessment, some design parameters are frozen, while the mission objectives, main geometric features, and operation conditions are varied. Table 5 shows the values of the frozen design parameters, which are derived from the design of Volocopter X2 and Joby S4. One of the crucial parameters of eVTOL design is the battery energy density. Projections of the energy density in the near and far future vary significantly and can largely influence the MTOM and performance of the vehicles. In this study, the value of 585 Wh/kg is selected based on the assumptions provided by the consortium involved in this research. This value corresponds to a far-future (projected 2050 entry year of operation) scenario in which the two architectures are expected to operate for both intra- and inter-city mobility, carrying 4 passengers (ranges above 50 km).

Parameter	Units	Multicopter	Tiltrotor
Number of PAX+Pilot	-	4+1	4+1
Battery energy density	Wh/kg	585	585
Wing span	m	NA	10.7
Horizontal tail volume coefficient	-	NA	0.70
Vertical tail volume coefficient	-	NA	0.04
Fuselage length	m	4.0	4.0
Number of propeller blades	-	2	5
Structural load factor	-	2.5	2.5
Landing gear height	m	1	1

Table 5 Main design parameters selected for the design of both vehicles.

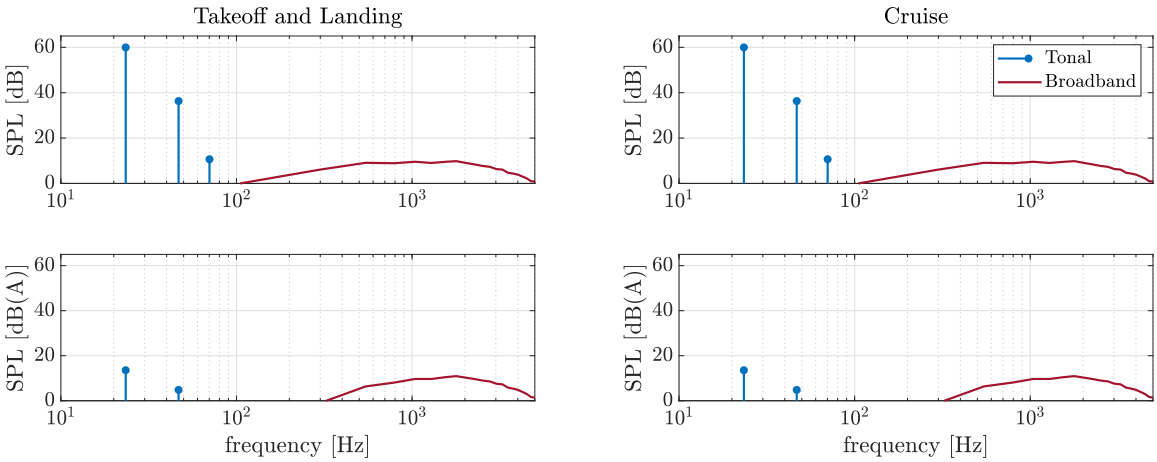

(a) Multicopter - takeoff and landing

(b) Multicopter - cruise

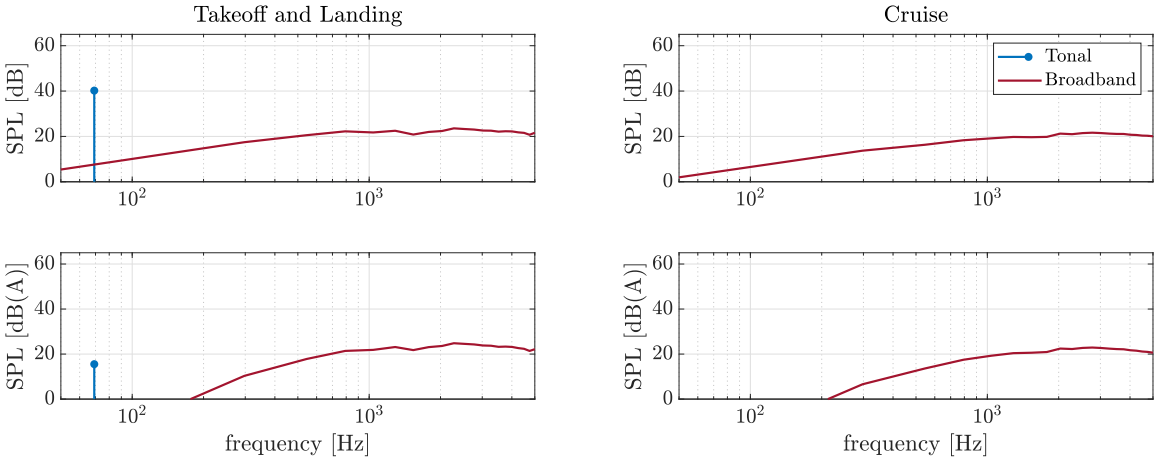

(c) Tiltrotor - takeoff and landing

(d) Tiltrotor - cruise

Fig. 5 Aircraft noise spectrum (Sound Pressure Level) in dB and dB(A) estimated 100 meters from the ground. Estimated tonal and broadband noise emissions from multicopter vehicle during takeoff and landing (a) and cruise, and from the tiltrotor vehicle during takeoff and landing (c) and (d) are shown.

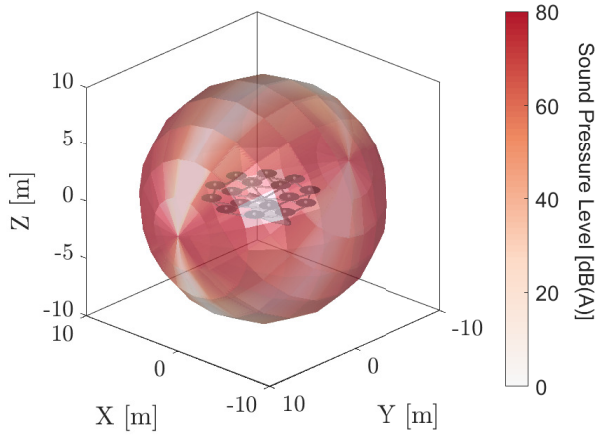

(a) Multicopter - cruise

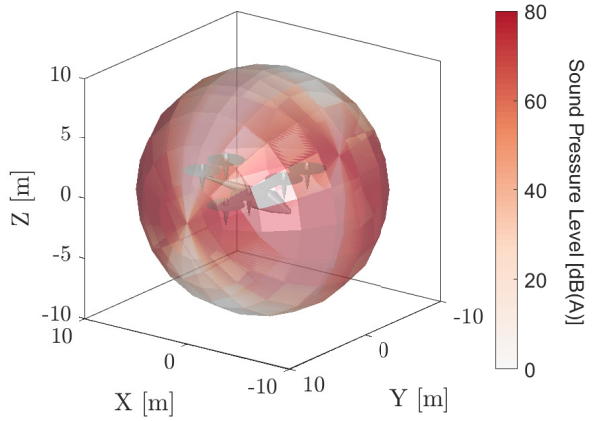

(b) Tiltrotor - takeoff and landing configuration

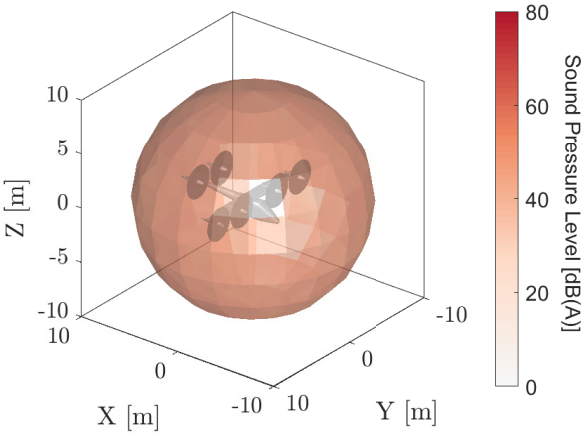

(c) Tiltirotor - cruise configuration

Fig. 6 Sound Pressure Levels captured 10 meters from the vehicles tested. (a) shows the noise from the multicopter vehicle in cruise configuration, and (a) and (b) show the tiltrotor vehicle in takeoff and landing and cruise configuration respectively.

In this study, the design exploration is performed over a design space, which is created by systematically varying a set of design variables across investigated architectures. The varied TLARs are the range, cruise speed, number of propellers, and wing area (for tiltrotors only). It is important to mention that the wing area is altered without modifying the aircraft span and, therefore, the wing area is inversely proportional to aspect ratio. The choice for fixing the wing span follows the importance of the vehicle dimension on the required infrastructure of vertiports. Table 6 highlights the range of the parameters varied and the increment given to each variation.

	Range R	V_{cruise}	N_{prop}	S
Units	km	km/h	-	[m^2]
Range of variable	25 - 300	50 - 250	6 - 18	10 - 26
Increment	25	50	4	4

Table 6 A summary of TLARs assessed for the design exploration.

The analysis starts by observing the performance of the two vehicle architectures depending on the choice of cruise speed and range. The criteria selected to filter the different number of propellers and wing areas is the energy consumption during the mission. The latter represents a standard performance-driven metric for aircraft design and reduces the dependency on assumptions such as energy cost and pilot rates. Figure 7 shows some performance parameters from the resulting best architectures with the lowest energy consumption for each range and assumed cruise speed. The figure on the left-hand side shows the performance indicator obtained for the multicopter architecture. The one in centre shows the performance indicator for the tiltrotor vehicle. The figure on the right-hand side shows which of the two yields the best performance on that particular indicator, with blue symbolizing the multicopter and red symbolizing the tiltrotor. The figures highlight the best points of operation for multicopters and tiltrotor architectures.

The general trend observed reveals that multicopter, as expected, are advantageous for short-range, low-speed operations, yielding lower total mass (MTOM), energy consumption during mission, and estimated operating costs for low-range and speed. Tiltrotor architectures, given the wing-based lift, are heavier at low speeds and short ranges due to the lower lift produced under these conditions and the extra weight of the wings. The tiltrotor design tool diverges under conditions of cruise speed lower than 100 km/h due to the extra energy required to sustain the aircraft during the cruise. Tiltrotor designs are more suitable for large ranges and high-speed conditions.

The MTOM estimations (first row of figures) indicate that multicopters outperform tiltrotor architectures even at speeds of 200 km/h at the smallest ranges tested (< 50 km). Nevertheless, this scenario is different when energy consumption or cost per PAX is analysed. Due to the different power requirements in cruise, tiltrotor architectures largely outperform the multicopter ones. The higher speed yields higher drag for the multicopter architecture, resulting in higher power consumption from the motors, which are used to lift the aircraft and overcome the drag forces. This is the opposite for the tiltrotor architecture, i.e. the higher cruising speeds yield higher lift, reducing the required power for the tiltrotors and compensating for the higher drag force. In this scenario, all conditions in which the vehicle is flying above 200 km/h are more suitable for tiltrotor architectures.

It is important to point out that the performance of the tiltrotor vehicle is highly dependent on the wing area from the design. Figure 8 shows the wing area that leads to the lowest energy required from the vehicle. Issues with the convergence of the method due to the required power at low speeds yield non-expected results for cruise speeds below 100 km/h. At lower speeds ($100 < V_{\text{cruise}} < 200$), the larger wing areas show optimal performance, mostly restricted by the maximum lifting force. At higher speeds, an opposite trend is observed. The flip in trend is attributed to the fact that the vehicle does not need the excessive lift offered by a wing with a large area. A smaller wing area yields a lower drag, thereby reducing the power required to cruise with an optimal lift-to-drag ratio.

Figure 9 highlights the noise emissions, in sound power level, stemming from the analysis shown in Figure 7. Here, two opposite trends are observed when comparing the noise emissions in takeoff and cruise. Takeoff emissions indicate that multicopter architectures are more advantageous under all conditions. This is attributed to the lower disk loading of multicopter architecture when compared to tiltrotor. The multicopter vehicle is lighter in most of the conditions at speeds lower than 150 km/h (Figure 7c), leading to a lower tip Mach number during takeoff. This observation, however, is completely reversed in cruising conditions, where tiltrotor emissions are greatly reduced, and are lower than the ones of the multicopter for all cruise speeds above 150 km/h. During the cruise, the power requirements of the tiltrotor vehicle are reduced significantly, commonly to less than 20% the one of takeoff. Conversely, a multirotor architecture requires higher power in cruise than in takeoff and landing. This indicator points to possible interesting decision conditions

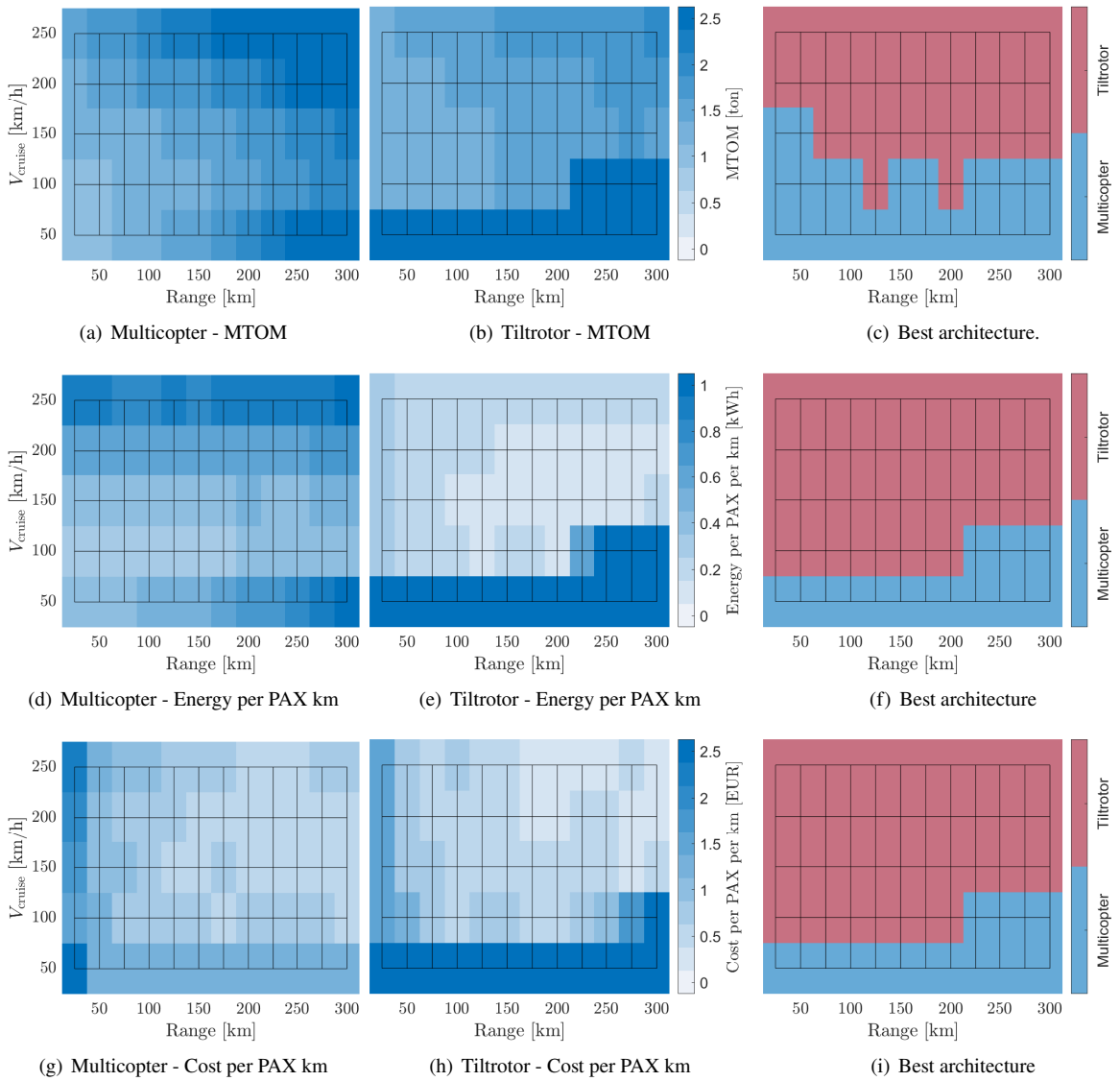

(a) Multicopter - MTOM (b) Tiltrotor - MTOM (c) Best architecture.

(d) Multicopter - Energy per PAX km (e) Tiltrotor - Energy per PAX km (f) Best architecture

(g) Multicopter - Cost per PAX km (h) Tiltrotor - Cost per PAX km (i) Best architecture

Fig. 7 Performance comparison between multirotor and tiltrotor vehicles designed for different ranges and cruise speeds. The designs are filtered with respect to minimum energy. Left-hand side pictures (a, d, and g) refer to the multicopter architecture. Centre figures refer to tiltrotor architecture (b, e, and h). Right-hand side pictures depict which of the architectures results in the best performance parameter. The first row of figures (a, b, and c) demonstrate the vehicle MTOM, the second (d, e, and f) the vehicle energy per PAX km, and the third (g, h, and i) the vehicle cost per PAX km.

when noise emissions are to be considered. At first, inter-city operations, within 50 km of range will possibly benefit from multicopter-like architecture. This follows the lower mass and, consequently, lower energy requirements, and noise emissions during cruise and vertical takeoff and landing. The noise emissions in the takeoff and landing part of the mission can also be relevant to facilitate the integration of vertiports in urban environments. For inter-city and long-range operations (>50 km), a tiltrotor vehicle is preferable when operating at speeds above 100 km/h. In such conditions, tiltrotor vehicles exhibit better performance than multicopters in terms of cruise speed, energy requirements, mission time, and noise emissions in cruise.

A summary of all previous findings is shown in Figure 10, whereas the characteristics of the vehicle with the lowest energy consumption per range are depicted. In this scenario, it is considered that, the cruise speed in which energy consumption during mission is the lowest is taken as the optimum design. The results of optimal cruise speed for the two

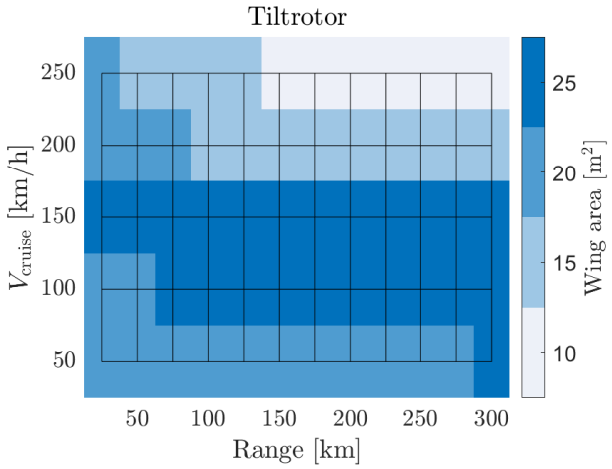

Fig. 8 Wing area of minimum energy tiltrotor configuration.

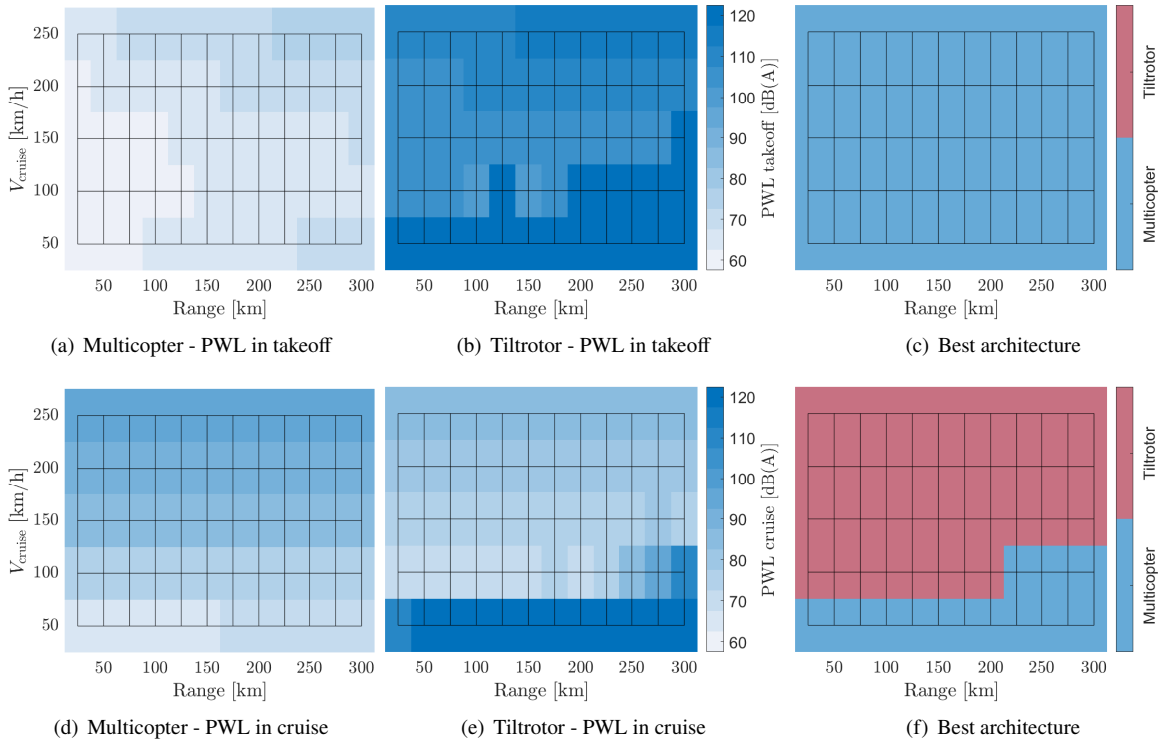

(a) Multicopter - PWL in takeoff (b) Tiltrotor - PWL in takeoff (c) Best architecture

(d) Multicopter - PWL in cruise (e) Tiltrotor - PWL in cruise (f) Best architecture

Fig. 9 Comparison of the sound power levels emitted by multirotor and tiltrotor vehicles designed for different ranges and cruise speeds in takeoff and landing conditions. The designs are filtered with respect to minimum energy. Right-hand side pictures depict which of the architectures results in the best performance parameter. The first row (a, b, and c) display the emissions in takeoff and the second row (d, e, and f) shows the emissions in cruise.

architectures (Figure 10a) show that the ideal operating speeds for the multicopter architecture are generally lower than the tiltrotor. In contrast, the cruising time (Figure 10b) of the multicopter architecture is higher than the tiltrotor one for most of the explored ranges, and the differences in time are seen to grow with extending the range, with an exception around 200-km range. The latter is an important blocker for employing multicopters for inter-city transportation, given that the comparable or higher speed of other means of transportation can negate the advantages of aerial transport.

Regarding the energy consumption per range (Figure 10d), different trends are observed for the multicopter and the tiltrotor. Multicopter architectures require heavier batteries to fly long distances, yielding significantly higher power. Therefore, a multicopter vehicle designed for a smaller range is more energy efficient. For a tiltrotor vehicle, an opposite result is observed, whereas the vehicle is more energy efficient when operating at long ranges. In this exploration, a minimum energy per km is obtained for a range of 200 km. At higher ranges, the extra battery required yields higher energy per km.

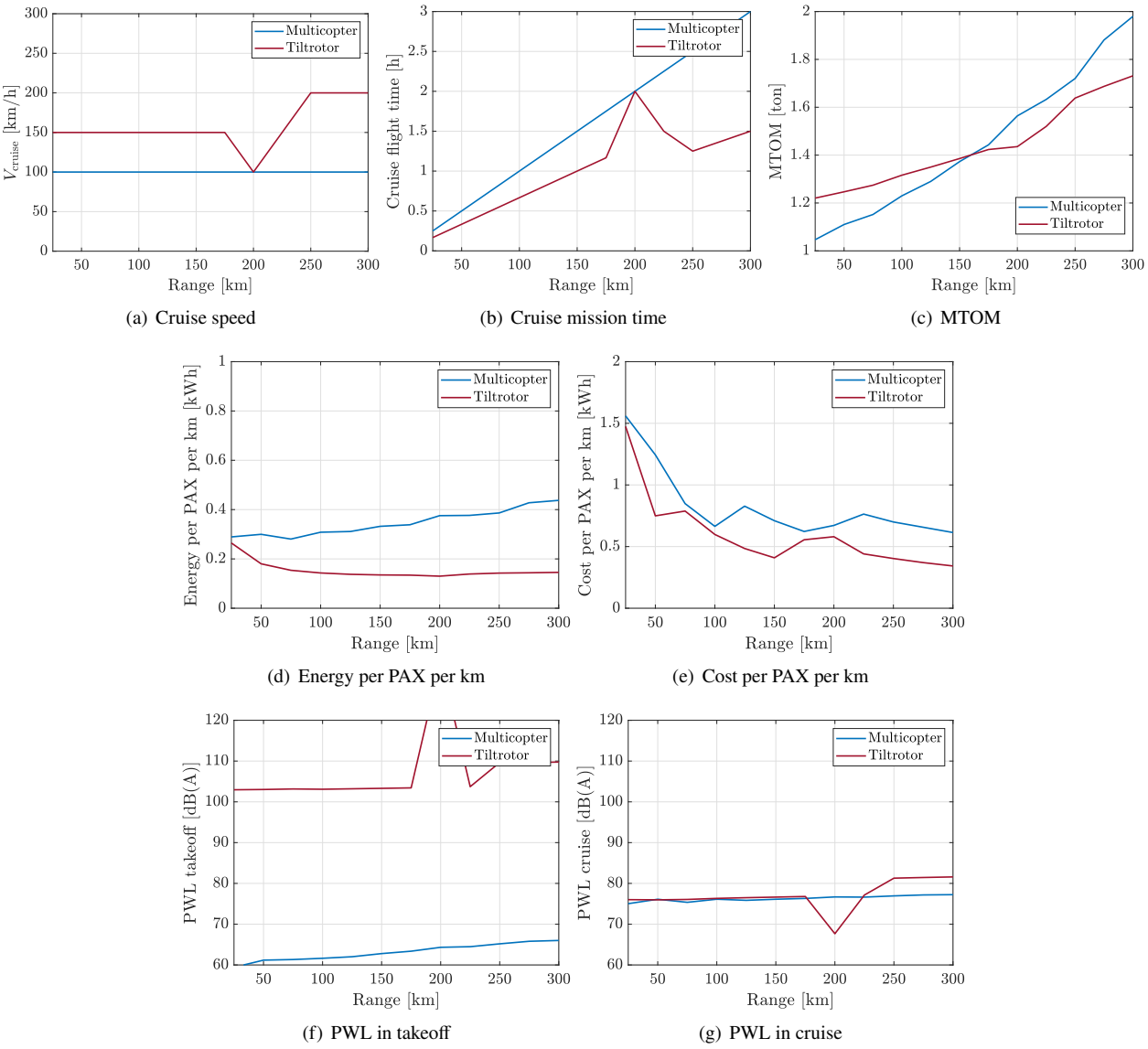

(a) Cruise speed (b) Cruise mission time (c) MTOM

(d) Energy per PAX per km (e) Cost per PAX per km

(f) PWL in takeoff (g) PWL in cruise

Fig. 10 Performance comparison of configurations with minimum energy per PAX per km for each analysed range. (a) shows vehicle optimum cruise speed, (b) mission time, (c) MTOM, (d) energy per PAX km, (e) cost per PAX km, (f) noise emissions in takeoff and landing, and (g) noise emissions in cruise.

A different result is seen when the operating cost is considered. The influence of indirect costs and pilot costs leads to lower costs per km for the highest ranges explored in all conditions and architectures. Tiltrotor architecture demonstrates lower energy, travel time, and estimated costs under all ranges. Nevertheless, the development of a tiltrotor vehicle is posed with secondary losses and risks that are not accounted for in this study, i.e. the transition between forward and vertical flight, the development of the tilting mechanisms, and the higher number of interconnected control systems. Collectively, these elements can significantly affect the vehicle's performance, particularly over short ranges,

resulting in underperformance compared to its multicopter counterpart.

Another crucial factor to consider is the noise emission of vehicles. As shown in Figure 10f, the level of noise emissions during takeoff for tiltrotor vehicles is significantly higher than multicopter vehicles, regardless of range. Across the explored ranges, the difference in sound power level between the two architectures is approximately 40 dB or higher. The results of cruise sound power level are demonstrated in Figure 10g. It is also of interest to note that the evaluated optimal vehicles of both architectures exhibit similar levels of noise during cruise. It is essential to note that the intended cruise speed of the tiltrotor is higher than the one of the multirotor architecture, yielding lower cumulative noise levels from the former.

V. Conclusions

This work is dedicated to the development and description of a design framework to be used for the assessment of performance and acoustic emissions of electric urban air mobility vehicles. A multidisciplinary tool is proposed to assess the aircraft mission performance and noise emissions, utilizing a set of high-level aircraft performance parameters. The evaluation of noise emission encompasses both tonal and broadband components and considers lumped forces and masses for each propeller. The tool comprises two different branches, enabling assessments for vehicles with both multicopter and tiltrotor architectures.

A preliminary evaluation of the tool is carried out using design parameters from existing vehicles. The resulting design architectures show performance indicators that are consistent with literature data of the existing vehicles, allowing a detailed discussion on the properties of the noise emission spectrum and directivity patterns of the two architectures investigated. The subsequent investigation focused on the exploration and comparison of the two architectures for a varying range of mission profiles and architectural choices. The results demonstrate the suitability of the two architectures for applications in urban environments. As expected, multicopter vehicles demonstrate higher power loading, due to the avoided extra mass of lifting elements, providing the best performance at low cruise speeds and small ranges. The cruise range is shown as the most critical aspect of multicopter architecture. Given the significantly higher power requirements during cruise than takeoff, operations in long ranges, e.g., inter-city commuting, are unlikely to be carried out. The corresponding feasibility relies on advancements in battery energy density. Conversely, advantages of tiltrotor architecture are mostly observed for high speeds and long ranges, where the fixed-wing-based lift leads to a cruise power much lower than that of the multicopter vehicles. Within the scope of this study, the ideal cruise speed is observed at around 200 km, where energy per km per passenger is minimized. The evaluation of noise emissions shows that the design preference for architecture varies according to operating conditions. Acoustic power levels during cruise are similar for both architectures. Nevertheless, the higher cruise speed of typical tiltrotor vehicles results in lower cumulative emissions to the urban environment. This comes at the price of significantly higher emissions during takeoff and landing, which adversely affects the overall noise emissions of tiltrotors, particularly over short ranges.

Overall, the results of this investigation highlight the importance of balancing energy efficiency, cost per trip, and noise emissions on the UAM market. The study also shows that the design choice of vehicle architecture has a high influence on these criteria. This study aims to demonstrate that a design framework capable of providing a holistic and quantifiable evaluation of vehicle design at preliminary design stages can assist choices of vehicle design and operation.

Acknowledgments

This study is funded by the European Union under Grant Agreement No. 101097120. Views and opinions expressed are however those of the author(s) only and do not necessarily reflect those of the European Union or CINEA. Neither the European Union nor the Granting Authority can be held responsible for them.

References

[1] "Vertical Flight Society eVTOL Aircraft Directory," , 2024. URL `https://evtol.news/aircraft`, Access date: 29-04-2024.

[2] NASA, "Urban Air Mobility (UAM) Market Study," Tech. rep., 2018.

[3] Rizzi, S. A., Huff, D. L., Boyd, D. D., Bent, P., Henderson, B. S., Pascioni, K. A., Sargent, C., Josephson, D. L., Marsan, M., He, H., and Snider, R., "Urban Air Mobility Noise: Current Practice, Gaps, and Recommendations," *Nasa/Tp-2020*, , No. October, 2020, p. 59. URL `http://www.sti.nasa.gov`.

[4] "European Union Aviation Safety Agency - EASA Drones & Air Mobility - Noise & Sustainability," , 2024. URL https://www.easa.europa.eu/en/domains/drones-air-mobility/drones-air-mobility-landscape/noise-sustainability, Access date: 29-04-2024.

[5] Magliozzi, B., Hanson, D., and Amiet, R. K., "Propeller and Propfan Noise," *Aeroacoustics of Flight Vehicles: Theory and Practice*, Vol. 1, 1991.

[6] Katz, J., and Plotkin, A., *Low-Speed Aerodynamics*, 2nd ed., Cambridge Aerospace Series, Cambridge University Press, 2001. https://doi.org/10.1017/CBO9780511810329.

[7] Drela, M., and Giles, M. B., "Viscous-inviscid analysis of transonic and low Reynolds number airfoils," *AIAA Journal*, Vol. 25, No. 10, 1987, pp. 1347–1355. https://doi.org/10.2514/3.9789.

[8] Roskam, J., *Airplane Design: Part 5-Component Weight Estimation*, DARcorporation, 1985.

[9] Hanson, D., "Propeller noise caused by blade tip radial forces," *10th Aeroacoustics Conference*, American Institute of Aeronautics and Astronautics, Reston, Virigina, 1986. https://doi.org/10.2514/6.1986-1892, URL https://arc.aiaa.org/doi/10.2514/6.1986-1892.

[10] Schlinker, R. H., and Amiet, R. K., "Helicopter Rotor Trailing Edge Noise," *NASA Contractor Report 3470*, 1981, p. NASA.

[11] Corcos, G. M., "Resolution of Pressure in Turbulence," *The Journal of the Acoustical Society of America*, Vol. 35, No. 2, 1963, pp. 192–199. https://doi.org/10.1121/1.1918431.

[12] Kamruzzaman, M., Bekiropoulos, D., Lutz, T., Würz, W., and Krämer, E., "A Semi-Empirical Surface Pressure Spectrum Model for Airfoil Trailing-Edge Noise Prediction," *International Journal of Aeroacoustics*, Vol. 14, No. 5-6, 2015, pp. 833–882. https://doi.org/10.1260/1475-472x.14.5-6.833.

[13] Hu, N., and Herr, M., "Characteristics of wall pressure fluctuations for a flat plate turbulent boundary layer with pressure gradients," *22nd AIAA/CEAS Aeroacoustics Conference, 2016*, 2016, pp. 1–18. https://doi.org/10.2514/6.2016-2749.

[14] Monteiro, F. d., Ragni, D., Avallone, F., and Sinnige, T., "Low-order acoustic prediction tool for estimating noise emissions from distributed propeller configurations," 2023. https://doi.org/10.2514/6.2023-4180.

[15] Brown, A., and Harris, W. L., "Vehicle design and optimization model for urban air mobility," *Journal of Aircraft*, Vol. 57, No. 6, 2020, pp. 1003–1013.

[16] Silva, C., Johnson, W., Antcliff, K. R., and Patterson, M. D., "VTOL urban air mobility concept vehicles for technology development," *2018 Aviation Technology, Integration, and Operations Conference*, 2018, pp. 1–16. https://doi.org/10.2514/6.2018-3847.

[17] Brown, A., and Harris, W. L., "Vehicle design and optimization model for urban air mobility," *Journal of Aircraft*, Vol. 57, No. 6, 2020, pp. 1003–1013. https://doi.org/10.2514/1.C035756.

[18] Maisel, M. D., Giulianetti, D. J., and Dugan, D. C., "The History of The XV-15 Tilt Rotor Research Aircraft: From Concept to Flight," *NASA Special Publication 4517*, 2000, p. 194.

[19] "Vertical Flight Society eVTOL Aircraft Directory - Volocopter 2X vehicle," , 2024. URL https://evtol.news/volocopter-2x/, Access date: 29-04-2024.

[20] "Vertical Flight Society eVTOL Aircraft Directory - Joby Aviation S4 vehicle," , 2024. URL https://evtol.news/joby-aviation-s4-production-prototype, Access date: 29-04-2024.